

Coherent short wavelength radiation via picosecond Nd:glass lasers

H. KURODA,¹ T. OZAKI,¹ A. ISHIZAWA,¹ T. KANAI,¹ K. YAMAMOTO,¹ R. LI² AND J. ZHANG³

¹Institute for Solid State Physics, University of Tokyo, 5-1-5 Kashiwanoha, Kashiwa, Chiba 277-8581, Japan

²Shanghai Institute of Optics and Fine Mechanics, P.O. Box 800-211, Shanghai 201800, P. R. China

³Institute of Physics, Chinese Academy of Sciences, P.O. Box 603, Beijing 100080, China

(RECEIVED 2 May 2001; ACCEPTED 11 October 2001)

Abstract

The generation of coherent soft X rays is studied using a terawatt picosecond Nd:glass laser system. Two different methods are investigated as candidates for efficient generation of such radiation, namely, longitudinally pumped transient collisional excitation nickel-like molybdenum X-ray laser, and high-harmonic generation from solid–vacuum interfaces. In the course of experiments on longitudinally pumped X-ray lasers, unexpected jetlike structures are observed in the visible emission of the molybdenum plasma, extending over a length of several millimeters. An interesting characteristic of this phenomena is that clear jets are observed only for longitudinal pump intensities between 5×10^{14} and 7×10^{14} W/cm². The effects of a finite scale length density gradient on surface harmonics is also investigated. The efficiency of harmonic generation from near-solid density plasma is found to increase by a factor of 2 to 3 when using prepulses. The scale length of the preplasma is simulated using a one-dimensional hydrodynamic code, and the increase in efficiency is verified to be in accordance with particle-in-cell simulation results.

Keywords: Harmonic generation; Plasma jet; Preplasma; X-ray lasers

1. INTRODUCTION

Scientists have strived to generate coherent sources of X rays using various methods, with high motivation for application in such areas as lithography, spectroscopy, and biological imaging. As a result, saturated nickel-like ion X-ray lasers with wavelengths between 13.9 and 20.3 nm have been generated using pump energies as small as 7 J (Dunn *et al.*, 2000), and capillary discharge technology has succeeded in developing high repetition rate extreme-ultraviolet lasers at 46.9 nm (Rocca *et al.*, 1994). Relatively large amplification of water-window X-ray lasers have been observed using huge fusion devices, and various works are now underway to reduce the energy requirement of such lasers for increased accessibility. There are, however, still many hurdles to clear before the X-ray laser technology matures enough for application research to flourish. One of the most important factors is a higher repetition-rate operation, which should be accompanied by shorter wavelengths and higher efficiency.

We are presently attempting to demonstrate a high-repetition rate coherent X-ray source by adopting two different methods. The first is longitudinal pumping of transient collisional-excitation X-ray lasers, where the high-intensity picosecond-duration main pulse pumps the preformed plasma from a longitudinal direction, rather than the transverse pumping used in conventional schemes. As a result of the smaller gain volume and the higher small-signal gain coefficient achieved in such pumping configurations, the total pump energy required for saturation is greatly reduced, and is about 250 mJ for the 18.9-nm nickel-like molybdenum laser. Another promising method for highly efficient generation of coherent soft X rays is harmonic generation from a solid–vacuum interface. Simulations (Gibbon, 1996) have shown that the conversion efficiency to the higher-order harmonics is a constantly increasing function of the pump laser intensity. Experiments using large Nd:glass lasers have demonstrated conversion efficiencies greater than 10^{-6} for harmonics up to the 68th order at 15.5 nm (Norreys *et al.*, 1996).

In this paper, we present results of our experimental investigations on the above two novel schemes of coherent soft X-ray generation. We will describe several interesting characteristics of the picosecond laser–plasma interaction

Address correspondence and reprint requests to the following present address: Tsuneyuki Ozaki, Ultrafast Optical Physics Group, Physical Science Laboratory, NTT Basic Research Laboratories, 3-1 Morinosato Wakamiya, Atsugi, Kanagawa 243-0198, Japan. E-mail: ozaki@will.brl.ntt.co.jp

revealed in these investigations. We will first give in Section 2 a short description of the high-peak-power picosecond laser system used in the present work. We will then present in Section 3 investigations of the interaction of a high-intensity picosecond laser pulse pumping a preformed plasma from a longitudinal direction. An unusually long jetlike emission from the plasma is observed, which extends over a length of 10 mm. A distinctive characteristic of the present phenomena is that it is only observed under longitudinal pump intensities between 5×10^{14} and 7×10^{14} W/cm². In Section 4, we investigate the effects of density gradients at the surface–vacuum interface on the conversion efficiency of surface harmonics. The optimum ratio and time interval between the intensity of the main pulse and prepulse is experimentally clarified. Simulations are performed, which show that the density gradients of the preformed plasma which results in the highest efficiencies are in accordance with predictions based on particle-in-cell simulation results of Lichters *et al.* (Lichters & Meyer-ter-Vehn, 1997).

2. LASER

In this work, we use the picosecond terawatt chirped pulse amplification laser system at the Institute for Solid State Physics of the University of Tokyo (Itatani *et al.*, 1996). A

schematic diagram of the layout of the system is shown in Figure 1. The master oscillator is a laser-diode-pumped mode-locked Nd:YLF laser (Lightwave model 131), which produces a stable train of 10-ps pulses at a wavelength of 1053 nm. These pulses are coupled into a 110-m-long, polarization-preserving single-mode fiber. With a combination of self-phase modulation and group-velocity-dispersion effects, the spectrum of the laser pulse is broadened and chirped. The high pointing stability and intensity stability of the laser-diode-pumped oscillator assures the stable operation of the whole system, which is especially important for a single-shot device. The chirped pulses are then sent to a folded two-pass stretcher equipped with one gold-coated holographic grating (Jobin-Yvon, 1740 l/mm). The temporal duration of the resulting pulse is stretched to 600 ps. A hard aperture is placed within the stretcher to limit the spectral bandwidth to 3 nm, which is necessary to keep the intensity of the pedestal low. The hard aperture is also used to match the central wavelength of the laser pulse to that of the gain bandwidth of the Nd:phosphate glass amplifier, at 1054 nm. The seed is then preamplified by a Ti:sapphire regenerative amplifier, which is pumped by the second harmonic of a Q-switched Nd:YAG laser. The typical output energy from the regenerative amplifier is 1 mJ, which is then sent through a four-pass 25-mm aperture flashlamp-pumped Nd:phosphate glass rod amplifier. For the longitudinally

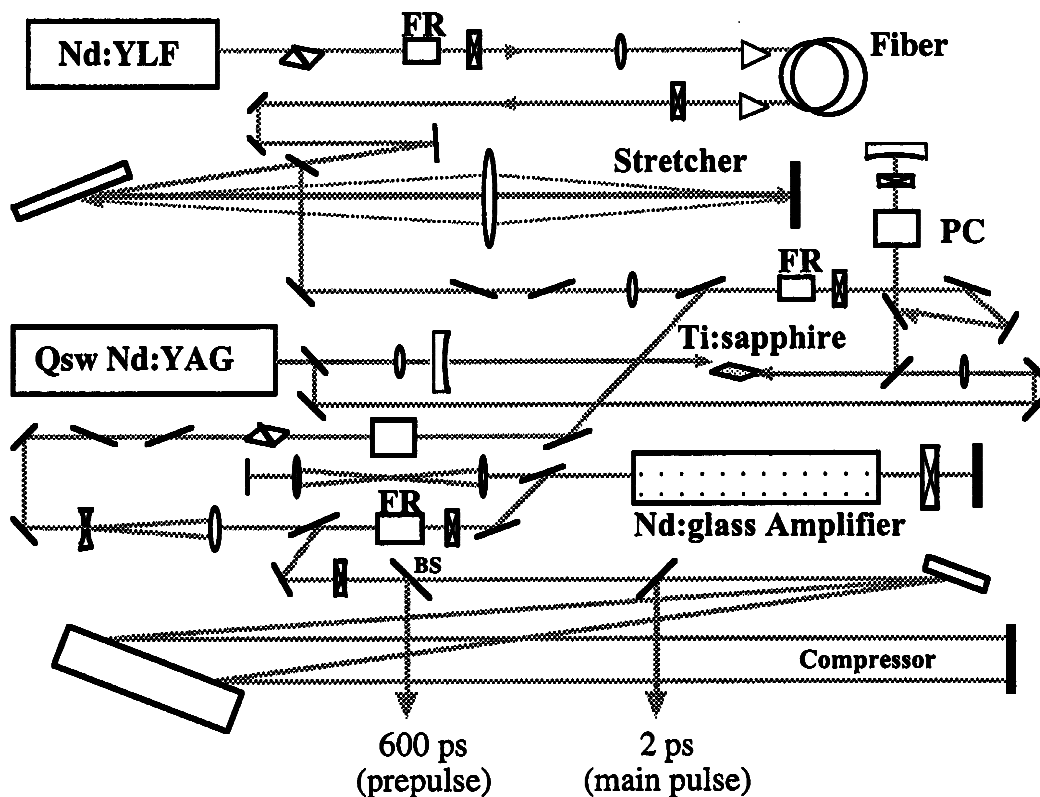


Fig. 1. Schematic diagram of the multiterawatt picosecond Nd:glass laser system.

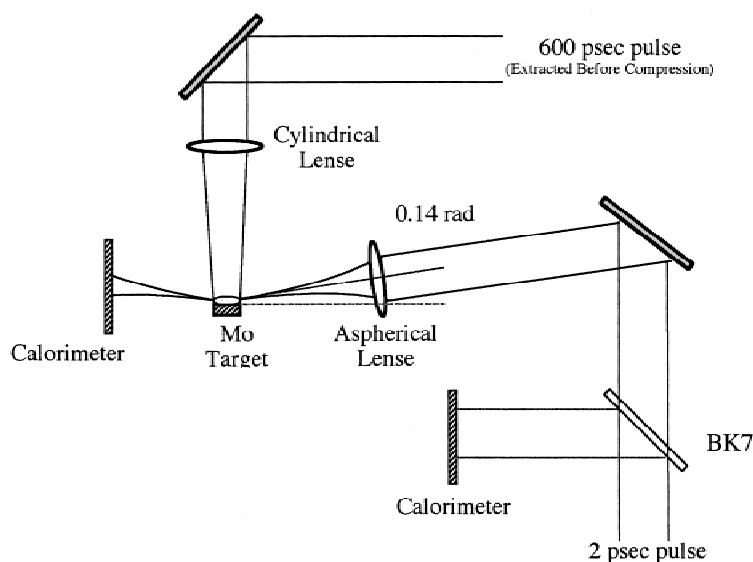


Fig. 2. Schematic diagram of the experimental setup in the vicinity of the target.

pumped X-ray laser experiments, the beam is then divided into two beams using a beam splitter. The reflected beam is used as a prepulse to produce the preformed plasma, while the transmitted beam is sent to a parallel grating pair compressor and compressed to a temporal duration of 2 ps. For surface harmonics experiments, compressed pulses are split into two beams to produce a picosecond prepulse. Large aperture Faraday isolators and a Pockel's cell is placed between the regenerative amplifier and the Nd:phosphate glass amplifier to increase the contrast ratio in the main pulse, and also to prevent amplified beams from returning to the vulnerable Ti:sapphire crystal and single-mode fiber. The contrast ratio between the pedestal to the main pulse is on the order of 10^{-6} , which is achieved mainly by spectral windowing. The maximum possible energy of the output from this system is 2 J, but it is usually operated at subjoule levels to prevent damage to the optics.

3. LONGITUDINALLY PUMPED TCE X-RAY LASERS

Figure 2 is a schematic diagram of our setup near the target vacuum chamber. The 600-ps prepulse is line-focused onto a 2-mm-long slab molybdenum target using a pair of cylindrical lenses. The 2-ps, p-polarized longitudinal beam is incident onto the preplasma at a grazing incidence angle of 0.14 rad. This angle is selected to maximize the propagation length of the picosecond laser through the preplasma, based on ray trace simulations. An $f/32$ aspherical lens is used to focus the longitudinal beam to a spot size of $140 \mu\text{m}$ at the entrance position of the preformed molybdenum plasma. Charge coupling devices (CCD) and PIN photodiodes observe the visible emission from the plasma, from a direction vertical to both the 2-ps beam and the 600-ps beam. These detectors are used to obtain the image and temporal

profile of visible emission from the laser-produced plasma. A 300-mm aperture calorimeter is also used to monitor the energy of the laser pulse after interaction with the molybdenum target or preformed plasma.

The transverse intensity profile of the longitudinal beam observed using a CCD camera after interaction with the preplasma is shown in Figure 3. Figure 3a is the picture observed for a simultaneous irradiation of both the prepulse and the main pulse. The peak intensity of the longitudinal and transverse beams are $8.0 \times 10^{14} \text{ W/cm}^2$ and $1.9 \times 10^{11} \text{ W/cm}^2$, respectively, and the peak-to-peak time delay between the main pulse and prepulse is 3.1 ns. The ordinate in

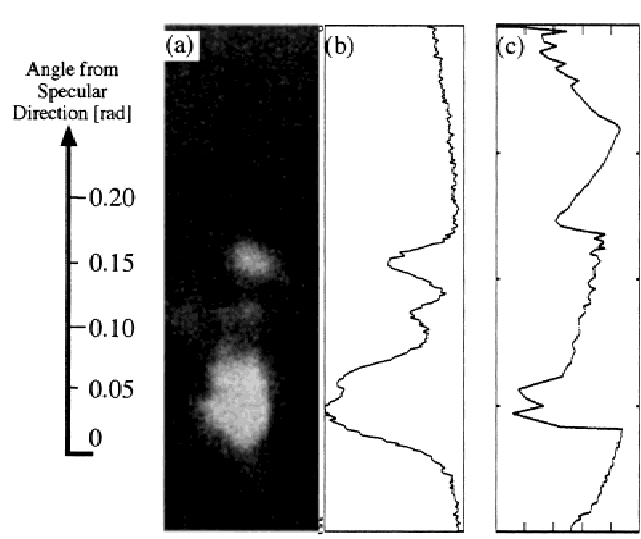


Fig. 3. (a) Transverse intensity profile of the transmitted longitudinal laser through preplasma. The intensity profile (b) is compared with simulation results (c).

Figure 3 corresponds to a direction vertical to the target surface, and the origin corresponds to the specular direction of the reflected longitudinal beam. We find that when the longitudinal beam travels through the preplasma produced by the transverse 600-ps laser, the beam profile on the negative angle side disappears, and instead a scattered pattern is observed at angles between 0.10 and 0.16 rad from the specular direction. The intensity of the transmitted beam is also considerably reduced compared with those observed without the prepulse.

Numerical simulations are performed to model the experimental observation, using a one-dimensional hydrodynamic code HYADES (Larsen & Lane, 1994) and a paraxial approximation ray tracing code. Outputs from the hydrodynamics code such as electron density, temperature, and average ionization are fed into the ray tracing code, which includes absorption of the incident laser based on the inverse bremsstrahlung effect. The experimental conditions such as pump intensity, temporal duration, and incidence angle are used as the input to the codes, without any artificial manipulations. Using the various outputs from these codes, we then calculate the angular intensity profile of the transmitted beam and compare the results with our experimental observations. In Figure 3c, we show the results of this simulation, and the experimentally observed profile is shown in Figure 3b. Although there are some differences in the position of the beamlets, the overall profile is excellently reproduced. When we look into the details of the simulation results, we find that the absence of the beam on the negative side of the specular direction is mainly due to defocusing of the beam, while the bright beamlets are the result of focusing of the beams after traveling through the preplasma.

Next we observed the visible emission from the plasma using a CCD camera. We show in Figure 4a the picture that was taken with an interference band-pass filter centered at a wavelength of 527 nm. The longitudinal beam enters from the left, and the transverse beam from the top, and the approximate position of the 2-mm-long Mo target is drawn in the figure. The peak intensity of the longitudinal beam in this case is 6.4×10^{14} W/cm². Interestingly enough, several jetlike emissions are observed, which exist over a length of

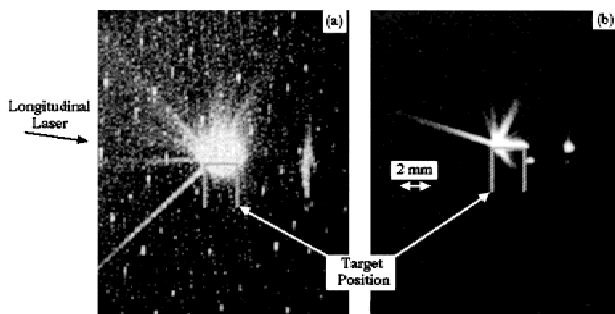


Fig. 4. Plasma emission in the visible wavelength observed with (a) a 527-nm band-pass filter, and (b) with additional neutral density filters.

several millimeters. Additional filters were added to decrease the fluence to the CCD, but the jetlike emission is still observed, as is shown in Figure 4b. When we irradiate the target with the 600-ps transverse pump only, no such jetlike emission is observed, even if the filters are reduced.

Next, with the shield left on, we observed the temporal profile of the plasma emission using a fast PIN photodiode. Scattered pump laser was eliminated by using a heat-absorbing filter. As a result, the emission is found to last for about 1 μ s, which is typical for visible emissions from a laser-produced plasma. From spectroscopic observations we find that the jetlike emission consists mainly of line emission from singly ionized and neutral Mo, and continuum emissions are relatively weak. Another interesting aspect of the present phenomena is that the jetlike emission is clearly observable only for a longitudinal pump intensity range between 5×10^{14} and 7×10^{14} W/cm². The actual cause for such jets is presently under investigation. However, this phenomenon may have some common mechanisms involved with a recently observed generation of massive plasma blocks moving toward the incident laser beam (Vogel & Kochan, 2001).

4. HARMONICS FROM A SOLID–VACUUM INTERFACE

Recent developments in generating ultrahigh peak power lasers (Perry & Mourou, 1994) have made possible a new range of experiments on laser–matter interactions. One of the most interesting phenomena is high-order harmonic generation from a solid surface. This method has attracted much attention because of the possibility of generating coherent X rays with wavelengths up to the water window at conversion efficiencies higher than those attainable with gas targets. Several experiments (Carman *et al.*, 1981a, 1981b; Kohlweyer *et al.*, 1995; von der Linde *et al.*, 1995, 1996; Norreys *et al.*, 1996; Zepf *et al.*, 1998; Földes *et al.*, 1999, 2000; Ishizawa *et al.*, 1999, 2000, 2001; Ganeev *et al.*, 2001) and theoretical results (Bezzarides *et al.*, 1982; Wilks *et al.*, 1993; Gibbon, 1996; Lichters & Meyer-ter-Vehn 1997) have been reported. Recently, the PIC simulation by Lichters *et al.* (1997) predicts that varying the density scale length L , which is produced when a high-intensity laser pulse irradiates the solid target, influences the harmonic emission. In an experiment, Zepf *et al.* (1998) showed that the harmonic efficiency depends strongly on the density scale length L/λ , where λ is the wavelength of the incident laser. Almost all previous experiments on harmonic generation from solid surfaces have been performed using a single pump pulse. In this work, we demonstrate a higher efficiency for harmonic generation by controlling the density scale length using double pulses. Harmonics of higher order are observed, and detailed model calculations are carried out using simulations.

The experiment was performed using the previously described chirped pulse amplification (CPA) Nd:glass laser system (Itatani *et al.*, 1996) for the driving laser. The 1054-nm

wavelength laser pulse is point focused onto an Al-deposited target within a vacuum chamber by using a 100-mm focal length achromatic lens. The incidence angle of the laser is 75° , the polarization of the driving laser is p-polarized, and harmonics generated from the plasma surface in the specular direction are spectrally dispersed by a monochromator and detected using a fast rise time photomultiplier. To modify the plasma scale length, we carried out experiments in which a 2.2-ps prepulse irradiates the solid target 0–20 ps prior to the arrival of the main Nd:glass laser pulse with the same pulse duration. Figure 5 shows the harmonic intensities of the third harmonics, when the prepulse intensity is (a) 0.04 and (b) 0.004 times that of the main pulse. We also show in the figure error bars corresponding to the standard deviation of the shot-to-shot variation in the harmonic intensity. Our present observations are limited up to the fifth harmonic. Although third harmonic radiation can also be observed when a single pulse is used (corresponding to the

data for 0 delay time), ~ 5 -ps time difference results in an increase in the harmonic signal by a factor of 2–3, which then decreases after 10 ps when the prepulse intensity is 0.04 times that of the main pulse. The results of the fourth and fifth harmonics are similar. The results for the fourth harmonics are of greatest importance because the even harmonics cannot be generated in a bulk of a preplasma, produced by amplified spontaneous emission or the pedestal. It is assumed that the divergence of a harmonic generated by irradiating double pulses is similar or larger than those generated by irradiating a single pulse, because the critical electron density surface will be more distorted for the former condition. Therefore, there is a possibility that the harmonic generation using the double pulses is more effective compared with that by single pulse irradiation.

On the other hand, the harmonic intensity for a single pulse (0 delay time) and double pulse irradiation is found to be smaller when the prepulse intensity is 0.004 times that of the main pulse. We can attribute this difference to the difference in the density scale length L/λ , produced when the laser pulse irradiates the solid target.

Figure 6 shows the density scale length L/λ as a function of the time difference between the main pulse and the prepulse, obtained from calculation using a 1D hydrodynamic code HYADES (Rubenchik *et al.*, 1998). When a high-intensity laser pulse is irradiated onto the solid target, the ponderomotive force acts on the target. As a result, density profiles initially resemble the step-shelf profiles (Estabrook & Kruer, 1978). We assume an upper shelf density n_0 of $27.5625 \times n_c$ in order to compare our result with the PIC simulation result of Lichters and Meyer-ter-Vehn (1997), where n_c is the critical density. We also assume that the plasma density increases linearly over a length from vacuum to the upper-shelf density. The gray zone in Figure 6 shows the optimum condition for the density scale length L/λ obtained from the PIC simulation result of Lichters *et al.* (1997). These calculation results show that harmonics are generated at a higher efficiency when the prepulse intensity is 0.04 times that of the main pulse, the time difference is ~ 5 ps, and the main pulse intensity is between $I\lambda^2 = 5 \times 10^{15}$ and $1 \times 10^{16} \text{ W} \cdot \text{cm}^{-2} \cdot \mu\text{m}^2$. This calculation result is in good agreement with our experiment results. As a result, it is found that the conversion efficiency of the harmonics does not strictly follow the $I\lambda^2$ scaling law, but rather depends strongly on the density scale length L/λ . A favorable density scale length L/λ depends on a trade-off between harmonics generated as a result of the strong light amplitude driving the free electron at the critical surface and the effect of resonance absorption. In the future, we plan to investigate the optimum double pulse irradiation condition combining both experiment and simulation.

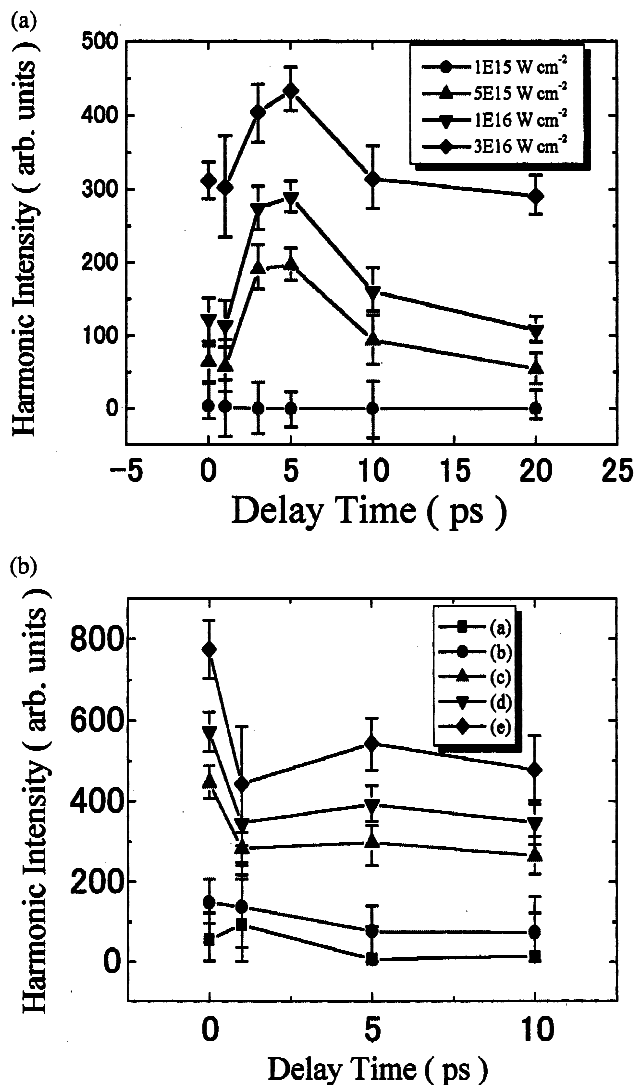


Fig. 5. The harmonic intensities of the third harmonics, when the prepulse intensity is (a) 0.04 and (b) 0.004 times that of the main pulse.

5. CONCLUSION

Investigations have been performed on the generation of coherent short wavelength radiation using picosecond

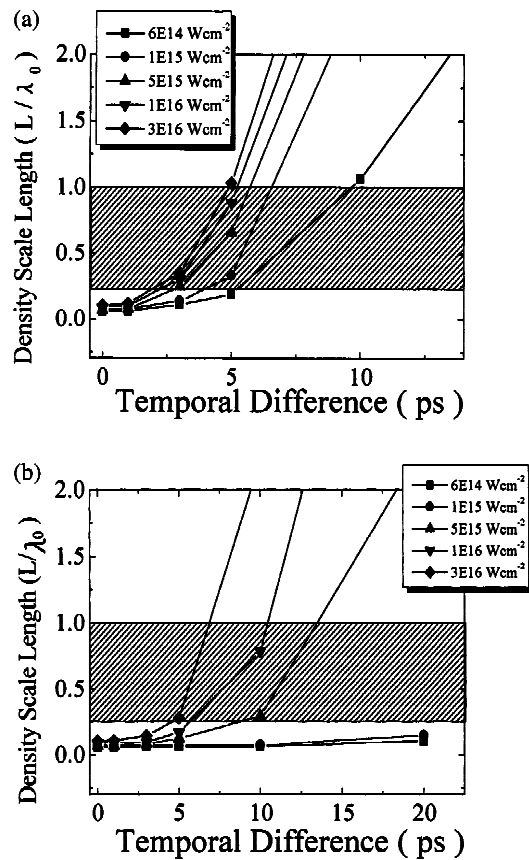


Fig. 6. The density scale length L/λ as a function of the time difference between the main pulse and the prepulse when the prepulse intensity is (a) 0.04 and (b) 0.004 times that of the main pulse. The gray zone shows the optimum condition for the density scale length L/λ from the PIC simulation result by Lichters and Meyer-ter-Vehn (1997).

Nd:glass lasers, and several new and interesting phenomena have been observed. Long jetlike structures in the visible emission have been unexpectedly observed, as a result of the interaction of a high-intensity laser interacting with a solid molybdenum target at an extremely oblique angle. The efficiency of harmonic generation from a solid–vacuum interface has been shown to increase by a factor of two to three, by using a low intensity prepulse to modify the density scale length. Investigations are presently underway to clarify the physics underlying these novel findings.

REFERENCES

- BEZZERIDES, B., JONES, R.D. & FORSLUND, D.W. (1982). Plasma mechanism for ultraviolet harmonic radiation due to intense CO_2 light. *Phys. Rev. Lett.* **49**, 202–205.
- CARMAN, R.L., FORSLUND, D.W. & KINDEL, J.M. (1981a). Visible harmonic emission as a way of measuring profile steepening. *Phys. Rev. Lett.* **46**, 29–32.
- CARMAN, R.L., RHODES, C.K. & BENJAMIN, R.F. (1981b). Observation of harmonics in the visible and ultraviolet created in CO_2 -laser-produced plasmas. *Phys. Rev. A* **24**, 2649–2663.
- DUNN, J., LI, Y., OSTERHELD, A.L., NILSEN, J., HUNTER, J.R. &

- SHLYAPTEV, V.N. (2000). Gain saturation regime for laser-driven tabletop, transient Ni-like ion X-ray lasers. *Phys. Rev. Lett.* **84**, 4834–4837.
- ESTABROOK, K. & KRUEER, W.L. (1978). Properties of resonantly heated electron distributions. *Phys. Rev. Lett.* **40**, 42–45.
- FÖLDES, I.B., BAKOS, J.S., BAKONYI, Z., NAGY, T. & SZATMÁRI, S. (1999). Harmonic generation in plasmas of different density gradients. *Phys. Lett. A* **258**, 312–316.
- FÖLDES, I.B., BAKOS, J.S., GÁL, K., JUHÁSZ, Z., KEDVES, M.Á., KOCSIS, G., SZATMÁRI, S. & VERES, G. (2000). Properties of high harmonics generated by ultrashort UV laser pulses on solid surfaces. *Laser Physics* **10**, 264–269.
- GANEV, R.A., CHAKERE, J.A., RAGHURAMAIAH, M., SHARMA, A.K., NAIK, P.A. & GUPTA, P.D. (2001). Experimental study of harmonic generation from solid surfaces irradiated by multipicosecond laser pulses. *Phys. Rev. E* **63**, 026402/1–6.
- GIBBON, P. (1996). Harmonic generation by femtosecond laser–solid interaction: A coherent “water-window” light source? *Phys. Rev. Lett.* **76**, 50–53.
- ISHIZAWA, A., INABA, K., KANAI, T., OZAKI, T. & KURODA, H. (1999). High-order harmonic generation from a solid surface plasma by using a picosecond laser. *IEEE J. Quantum Electronics* **35**, 60–65.
- ISHIZAWA, A., KANAI, T., OZAKI, T. & KURODA, H. (2000). The spatial distribution of high-order harmonics from solid surface plasmas. *IEEE J. Quantum Electronics* **36**, 665–668.
- ISHIZAWA, A., KANAI, T., OZAKI, T. & KURODA, H. (2001). Enhancement of high-order harmonic generation efficiency from solid surface plasma by controlling the electron density gradient of a picosecond laser produced plasmas. *IEEE J. Quantum Electronics* **37**, 384–389.
- ITATANI, J., KANAI, T., OZAKI, T. & KURODA, H. (1996). Nd:glass and Ti:sapphire hybrid short pulse laser system. *Prog. Cryst. Growth Charact. Mater.* **33**, 281–284.
- KOHLWEYER, S., TSAKIRIS, G.D., WAHLSTRÖM, C.G., TILLMAN, C. & MERCER, I. (1995). Harmonic generation from solid–vacuum interface irradiated at high laser intensities. *Opt Commun.* **117**, 431–438.
- LARSEN, J.T. & LANE, S.M. (1994). HYADES—A plasma hydrodynamics code for dense plasma studies. *J. Quant. Spectrosc. Radiat. Transf.* **51**, 179–186.
- LICHTERS, R. & MEYER-TER-VEHN, J. (1997). High laser harmonics from plasma surface: Intensity and angular dependence, cutoffs and resonance layers at density ramps. *Inst. Phys. Conf. Ser.* **154**, 221.
- NORREYS, P.A., ZEPF, M., MOUSTAIZIS, S., FEWS, A.P., ZHANG, J., LEE, P., BAKAREZOS, M., DANSON, C.N., DYSON, A., GIBBON, P., LOUKAKOS, P., NEELY, D., WALSH, F.N., WARK, J.S. & DANGOR, A.E. (1996). Efficient extreme UV harmonics generated from picosecond laser pulse interactions with solid targets. *Phys. Rev. Lett.* **76**, 1832–1835.
- ROCCA, J.J., SHLYAPTEV, V., TOMASEL, F.G., COTÁZAR, O.D., HARTSHORN, D. & CHILLA, J.L.A. (1994). Demonstration of a discharge pumped table-top soft X-ray laser. *Phys. Rev. Lett.* **73**, 2192–2195.
- RUBENCHIK, A.M., FEIT, M.D., PERRY, M.D. & LARSEN, J.T. (1998). Numerical simulation of ultra-short laser pulse energy deposition and bulk transport for material processing. *Appl. Surf. Sci.* **129**, 193–198.
- VOGEL, N.I. & KOCHAN, N. (2001). Experimental investigation of stochastic pulsation and formation of light bullets with mega-

- gauss magnetic fields by an intense laser pulse propagating in a preionized plasma. *Phys. Rev. Lett.* **86**, 232–235.
- VON DER LINDE, D., ENGER, T., JENKE, G., AGOSTINI, P., GRILLON, G., NIBBERING, E., CHAMBARET, J.-P., MYSYROWICZ, A. & ANTONETTI, A. (1996). Generation of ultrashort XUV pulses by harmonic generation from solid surfaces. *SPIE* **2770**, 98–105.
- VON DER LINDE, D., ENGER, T., JENKE, G., AGOSTINI, P., GRILLON, G., NIBBERING, E., MYSYROWICZ, A. & ANTONETTI, A. (1995). Generation of high-order harmonics from solid surfaces by intense femtosecond laser pulses. *Phys. Rev. A* **52**, R25–27.
- WILKS, S.C., KRUEER, W.L. & MORI, W.B. (1993). Odd harmonic generation of ultra-intense laser pulses reflected from an overdense plasma. *IEEE Trans. Plasma Sci.* **21**, 120–124.
- ZEPF, M., TSAKIRIS, G.D., PRETZLER, G., WATTS, I., CHAMBERS, D.M., NORREYS, P.A., ANDIEL, U., DANGOR, A.E., EIDMANN, K., GAHN, C., MACHACEK, A., WARK, J.S. & WITTE, K. (1998). Role of the plasma scale length in the harmonic generation from solid targets. *Phys. Rev. E* **58**, R5253–5256.